In-Situ Observations of Jetting in the Divergent Rebound Regime for High-Velocity Metallic Microparticle Impact

Yuchen Sun[1,2,3], David Veysset[1], Keith A. Nelson[1,2], and Christopher A. Schuh[3,a)]

[1]Institute for Soldier Nanotechnologies, Massachusetts Institute of Technology, Cambridge, Massachusetts 02139, USA.
[2]Department of Chemistry, Massachusetts Institute of Technology, Cambridge, Massachusetts 02139, USA.
[3]Department of Materials Science and Engineering, Massachusetts Institute of Technology, Cambridge, Massachusetts 02139, USA.

a) Author to whom correspondence should be addressed: schuh@mit.edu

Abstract

Metallic bonding of certain materials can be achieved via high-velocity impact, and this type of bonding is often linked to an intense extrusion of material from the impact site, known as jetting. We present *in-situ* observations of hydrodynamic jetting and ejection of matter from high-velocity metallic microparticle impacts that still result in rebound of the particle. While the occurrence of jetting has been linked to permanent particle deposition in prior studies, the present findings reveal that any bonds that may form upon jetting can be rebroken by particle rebound in some circumstances. We further present asymmetric occurrences of jetting associated with localized delays in particle detachment followed by rotation during particle rebound, which may speak to transient bond formation at the jetting sites.

Impacts between metallic microparticles and substrates at sufficiently high velocities will result in bonding between the two bodies for certain materials and conditions[1–5]. This impact-induced metallic bonding is the foundation of particle deposition in spray-coating processes such as cold spray and micro-additive manufacturing methods including laser-induced forward transfer[6,7]. The mechanisms responsible for such particle deposition are of great interest, but not yet firmly established. One phenomenon closely associated with successful particle deposition is the process of hydrodynamic jetting—an intense, splash-like extrusion of solid material from the particle-substrate interface[8–10]. Post-impact observations and simulations suggest jetting can provide the pristine and intimate contact required for metallic bonding[11–13], disrupting surface oxide or contamination layers and permitting metal-on-metal contact.

Jetting events take place over a matter of nanoseconds and at scales at and below one micrometer, and are therefore difficult to study directly. As a result, this phenomenon is the subject of much inference and speculation. In particular, the connection between jetting and bond formation has largely studied 'bonding' as a simplified binary yes/no condition speaking to whether the particle rebounded or not. Such characterization does not precisely reflect the onset of metallurgical bonding, but rather the threshold required for permanent particle deposition. Post-impact observations of particle-substrate interfaces in such deposited particles clearly demonstrate a spectrum of bonding degree[9,10,14,15]. The paucity of direct observations of jetting events leading to bonding leaves a knowledge gap about the mechanism of bonding, so the link between jetting and bond formation remains the subject of debate[5,16–20].

There are only a few published cases of *in-situ* jet observation: those from our group's work on Al[21] and Au[22] particles at velocities where the particles permanently adhered upon impact, above the so-called 'critical velocity' for particle adhesion. Recently, we presented post-impact observations suggesting that jetting occurred in some rebounding impacts, which may speak to the formation of transient bonds which are broken upon rebound, and which cause a divergence from typical power-law rebound behavior[23]. However, no *in-situ* evidence of jetting, like that for deposited Al and Au particles, has been captured for rebounding impacts. This results from a combination of factors. First, it is difficult to reliably access the small range of particle velocities within which both jetting and rebound occurs. Second, a diminishingly small amount of jetting is expected in this range and it is very short-lived, spanning just nanoseconds even under favorable conditions. Finally, the length scale of this phenomenon is very small, with the width of jets near the limit of what can be imaged with visible light. Accordingly, in this paper, we present a campaign of high time-resolution experiments in the range of velocities near the bonding threshold where transient bond formation and rupture might be observed. As a result of these experiments, we present *in-situ* observations of jetting events for impacts resulting in rebound and provide direct confirmation of the link between divergent rebound behavior and jetting events.

High-velocity microparticle impacts were performed with the laser-induced particle impact test (LIPIT) platform[24–26]. For each impact, a single microparticle was selected and accelerated towards a target. Details regarding particle launching can be found in previous publications[21,27]. In this study, we present

impacts of atomized spherical aluminum particles with a nominal size of 31 μm from Valimet (Stockton, USA) on aluminum substrates of thickness 3.175 mm from OnlineMetals (Seattle, USA). Substrate surfaces were ground and polished to a nominal 0.04 μm finish prior to impact experiments. The impact events were captured through a microscope objective by an ultra-high frame rate camera consisting of 16 independently triggered intensified CCD cameras. This camera allows capture of images with as little as 5 nanoseconds between frames. Fig. 1 is a representative image sequence of nine select frames showing the impact and subsequent rebound of an Al microparticle from an Al substrate. From these images, the impact and rebound velocities are measured to be 360 and 32 m/s respectively. The coefficient of restitution (COR), defined as the ratio between rebound and impact velocities, is 0.089. Additionally, we observe that the rebounding particle slightly rotates; in the projected plane it has an angular velocity of 2×10^5 rad/s. This may result from various imperfections on either the particle or the substrate surface, or in the microstructure of the metal in the impact zone.

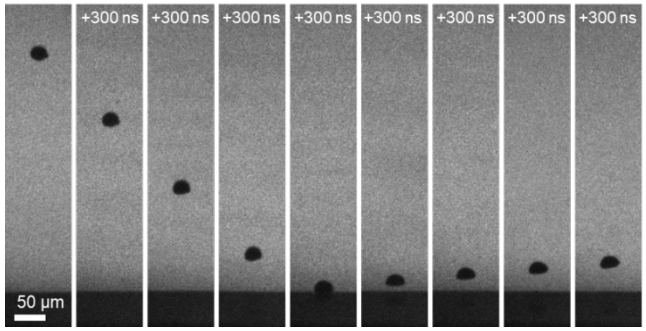

Fig. 1. An image sequence showing an aluminum microparticle (28 μm diameter) impacting an aluminum target at 360 m/s and rebounding at 32 m/s.

Fig. 2(a) presents a collection of impact data for aluminum microparticles impacting aluminum over a range of impact velocities. We combine impact data presented previously[21] (30 ± 7 μm diameter) with those collected specifically for this study (30 ± 3 μm diameter) to demonstrate that the experiments are comparable and not anomalous. These impact data are redisplayed on a double logarithmic scale in Fig. 2(b), and, following a similar analysis performed by us previously[23], we observe two regimes of rebound behavior below the critical velocity for particle deposition. At low to moderate impact velocities, the behavior agrees with a well-established rebound power law, $\mathrm{COR} \propto V_i^{-1/2}$, put forth to model elastic-perfectly plastic (EPP) rebound behavior[28,29]. At higher velocities approaching the deposition threshold, we observe a regime of divergence from that power law[23].

The interframe times in most impacts presented in Fig. 2 (e.g., 300 ns in Fig. 1) are optimized to reduce uncertainty in velocity measurements. However, this substantially reduces the likelihood of observing rapid events such as jetting, which appear for a few tens of nanoseconds. Therefore, the present campaign focused specifically on the regime of power-law divergence in Fig. 2(b), and involved either detailed microscopic examination of post-impact sites, more highly resolved videography focused on the time interval around the impact event itself, or both. Figs. 2(c)–(f) correspond to images of craters resulting from impacts at 660, 685, 700, and 660 m/s, respectively, all of which lie within the divergent rebound regime, as indicated on Fig. 2(b). These impacts resulting in particle rebound all show post-impact evidence of jet formation, including extruded material at the crater rim and even narrow ruptured

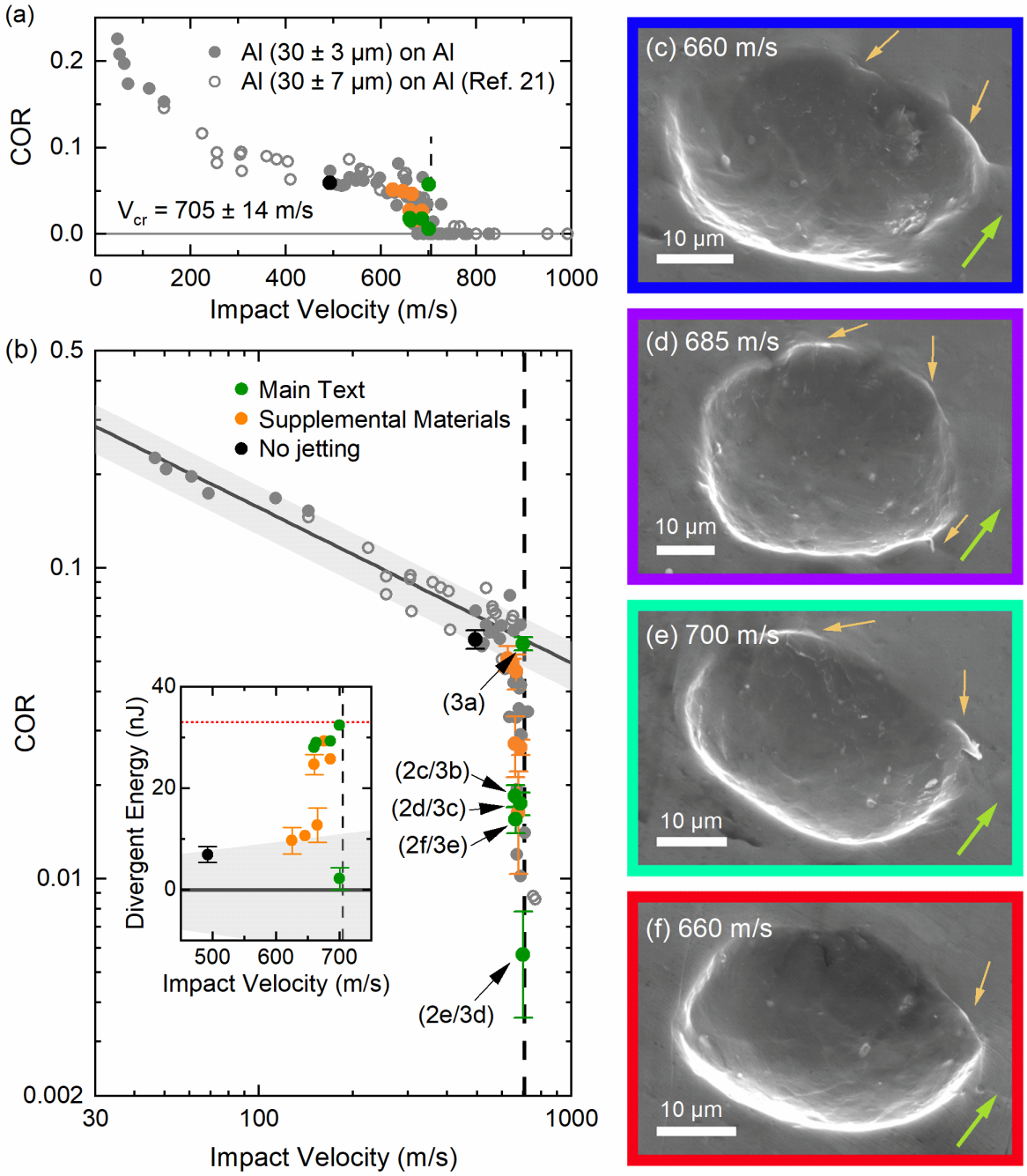

Fig. 2. (a) Coefficients of restitution (COR) versus impact velocity (V_i) for aluminum microparticle impacts on aluminum are shown on linear axes and **(b)** double-logarithmic axes. A power law fit is shown for COR ∝ $V_i^{-1/2}$ with divergent behavior observed as V_i approaches the critical velocity. The inset shows divergent energy, i.e., the additional energy lost that is not predicted by the power law, in the impact velocity range leading up to bonding. Gray regions correspond to a 95% confidence interval for the power law fit and the red dotted line denotes the divergent energy associated with the bonded state at the critical velocity. Post-impact SEM images of the target surface show formation of incipient jets despite particle rebound for impacts at **(c)** 660 m/s, **(d)** 685 m/s, **(e)** 700 m/s, and **(f)** 660 m/s. The four images shown in (c)–(f) correlate to the sequences in Figs. 3(b)–(e), respectively, denoted by the color frames. The green arrows denote a common direction in the laboratory frame here and in Fig. 3.

material that sticks up from the surrounding surface and appear torn, as though heavily plastically deformed to a local failure event. Such signals of jetting around craters have been seen in our prior LIPIT work on copper[23]. Sites showing signs of jetting reported in the main text, i.e., those in Figs. 2(c)–(f) and Fig. 3, are marked in green in the COR plots of Fig. 2. Sites with observations of jets reported in Fig. S1 are marked in orange. Measurement errors are approximated by the size of the points unless explicitly shown. One site with no signs of jetting was observed for an impact at 492 m/s; this point is marked in black, with the corresponding SEM in Fig. S2.

One common feature of the microscopic observations in Fig. 2 and in prior work[11,23] is that the presence of a legitimate 'jet' vis-à-vis a pronounced conventional pile-up around in the impression site is somewhat subjective; these are indirect inferences about the occurrence of jetting, and they have associated uncertainty. We therefore proceed to examine *in-situ* observations of impacts in Fig. 3, which correspond to the craters presented in Fig. 2 but can provide direct evidence of jetting in such rebounding cases. These image sequences have only 15 or 20 ns between frames during particle-substrate contact, revealing in detail events during the contact duration. The *in-situ* sequences shown in Figs. 3(b)–(e) correspond to the post-impact craters shown in Figs. 2(c)–(f), respectively. We are further able to spatially correlate the *in-situ* and post-impact observations by cross-comparing the two figures, noting that the green arrows point in the same direction in the laboratory frame for both presentations.

Importantly, in each of the sequences in Fig. 3(a)-(d), we identify with arrows events of material ejection from impacts resulting in particle rebound. These *in-situ* jetting events are not as clear as those presented previously for non-rebounding particles[21]; the amount of jetted material is certainly lower in these rebounding impacts. Trimmed and enlarged versions of Fig. 3(b)-(d) are presented in Fig. S3 to better indicate the jetting events. What is more, in Figs. 3(a), 3(c), and 3(d), jetting is observed only on one side of the particle but not the other, whereas for bonding particles, jetting was observed on both sides of the particle[21]. In Fig. 3(a), jets form only on the left side of the particle. Further, as the particle subsequently rebounds, the right side of the particle detaches first, with the left side remaining in contact with the substrate. This in turn results in substantial rotation of the particle as it rebounds with an angular velocity of $2\text{x}10^6$ rad/s, one order of magnitude greater than the rotation observed in Fig. 1. Similar rotating rebounds are also observed in Fig. 3(c) and 3(e) with angular velocities of $5\text{x}10^5$ rad/s, and $6\text{x}10^5$ rad/s, respectively, again more than twice that seen in the non-jetting case of Fig. 1. In Fig. 3(b), where jetting is observed on both sides of the particle, the corresponding angular velocity is $2\text{x}10^5$ rad/s, comparable to the rotation measured following a non-jetting impact. Angular velocities of select impacts are displayed versus impact velocity in Fig. S4, which further depict the marked increase in rotation associated with jetting impacts.

In cases like these where jetting is observed *in-situ*, we can further examine the corresponding craters, where we identify post-impact jetting on the same side of the impact crater where the jet was observed *in-situ*. For example, the SEM image in Fig. 2(d) shows jetting in the direction parallel to the arrow, correlating with the direction of ejection in Fig. 3(c). This conformity validates that such observations are indeed associated with jetted and ejected matter. In Fig. 3(e), while no ejection is observed, there is substantial rotation during rebound, with some component in the out-of-page direction. Based on the

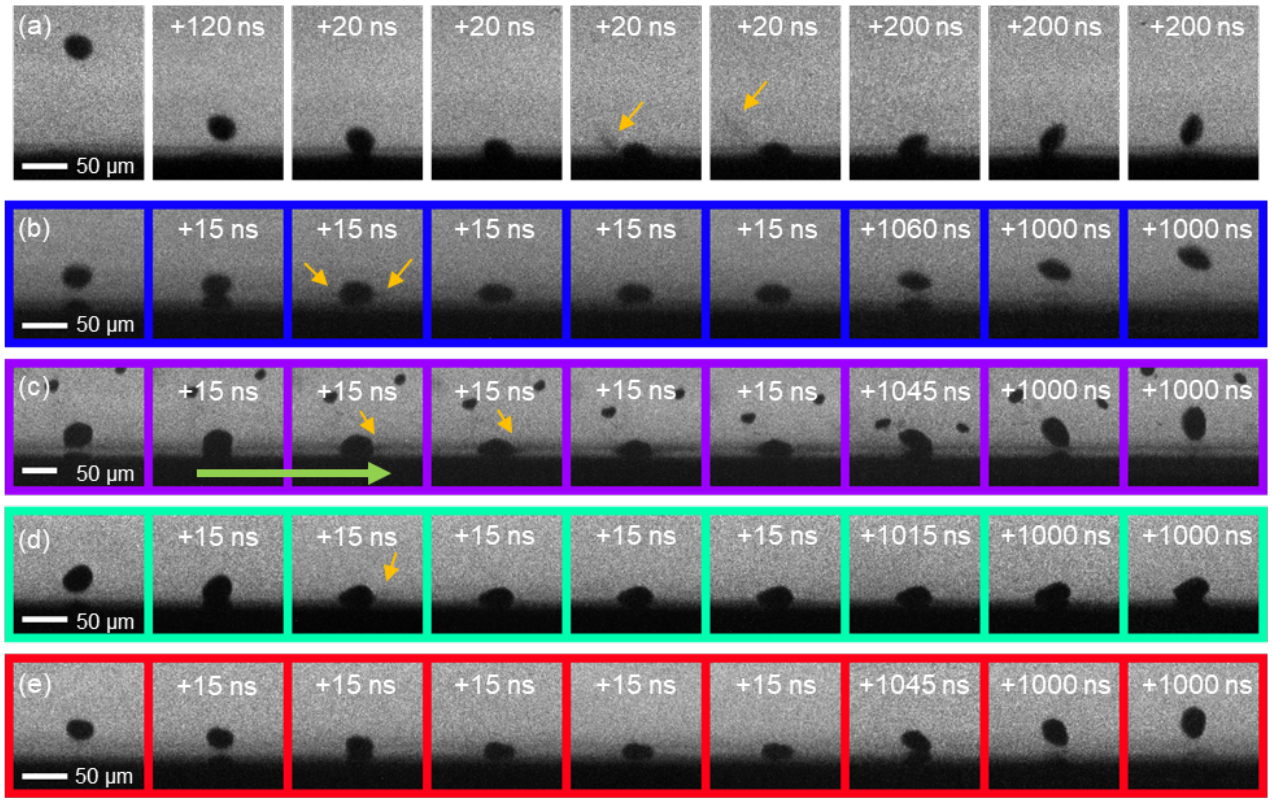

Fig. 3. *In-situ* observations of aluminum particles impacting aluminum at **(a)** 700 m/s, **(b)** 660 m/s, **(c)** 685 m/s, **(d)** 700 m/s, and **(e)** 660 m/s. The yellow arrows highlight material jet initiation or full ejection from the particle-substrate interface. The sequences in Figs. 3(b)–(e) correlate to the images in Fig. 2, denoted by the color frames. The green arrow denotes the laboratory frame direction for Figs. 3(b)–(e) corresponding with the green arrows in Fig. 2.

similar rebound rotation observed in Figs. 3(a) and (c), this suggests that jetting may have occurred but was not captured in the sequence, possibly occurring in the 15 ns time window between frames. The matching SEM in Fig. 2(f) corroborates this speculation, as it shows jetting in a direction not directly parallel to the green arrow, corresponding to the rotation, suggesting that material ejection during the impact would likely have been obscured by the particle itself and less likely to be observed.

In our prior work, we observed the power-law divergence and associated it with microscopic evidence of jets for copper-on-copper impacts[23]. The above observations not only provide post-impact evidence for a second material, aluminum, but *in-situ* evidence which provides a clean and direct confirmation that power-law divergence is associated with jetting. The excess lost energy in the divergence regime, i.e., the rebound kinetic energy that is not accounted for by just the elastic-plastic deformation required to flatten the particle and create the impact crater, is shown for select data in the Fig. 2(b) inset. At the critical velocity, the divergent energy corresponds to the energy associated with the particle permanently adhering to the substrate[23,30], which, in the present case, is about 30 nJ, denoted by the horizontal dotted line in the Fig. 2(b) inset.

In our previous paper, we proposed two mechanisms for the power-law divergence based on the emergence of jetting there: (i) kinetic energy loss via ejected material and (ii) the refracturing of transient metallic bonds formed between particle and substrate[23]. The present observations introduce a third component to this energy balance—rotational kinetic energy. For the rebounds shown in Figs. 3(c) and (e) we estimate the rotational kinetic energy as being close to the error level on the divergence energy, less than 1 nJ. (We measure the particle's rotational velocity directly and use the rotational kinetic energy formula for an oblate spheroid, whose dimensions we also obtain from the *in-situ* images.) For the impact in Fig. 3(a), we estimate the rotational kinetic energy to be ~10 nJ, which is significant compared to the ~30 nJ divergent energy associated with particle deposition. However, in no case is the rotational energy enough to explain fully the extra loss of energy in the run-up to bonding. Accordingly, it is likely that our previously postulated mechanisms remain relevant.

One of the proposed mechanisms of energy loss in the divergent regime is the formation of some transient bonds where jetting occurs, which are insufficient to keep the particle from rebounding and refracturing those bonds. We note that our present observations may provide some support for that mechanism. Figs. 3(a) and 3(c) both show an asymmetrical jetting event associated with a localized delay in particle detachment on the corresponding side, followed by particle rotation during rebound. From these series of observations, the particle appears to "tear away" from a possible attachment point associated with the jetted region. However, other sources of asymmetry and rotation can certainly be imagined, including irregularities in the particle shape or microstructure, etc. While the current observations suggest an interpretation in terms of transient bonding, further investigation into finer details of the crater morphology, and possibly captured particles after rebound, as well as impacts between mismatched material systems may help further confirm the occurrence of transient bonding through identification of fresh fractured regions; we hope to address this in future work.

To summarize, our *in-situ* observations provide direct support for an earlier conjecture that in metallic microparticle impact, hydrodynamic jetting sets on and depletes kinetic energy from an impacting particle even below the critical velocity required for permanent particle adhesion. This result implies that successful particle deposition requires a sufficiently extensive amount of jetting, which has been suggested as a precursor to the formation of metallic bonds. Our observation of asymmetric jetting followed by a rotating particle rebound may indeed further link jetting with bond formation, the resulting bonds being transient and re-broken in the rebounding particles.

Acknowledgments

This work was primarily supported by the U.S. Department of Energy, Office of Science, Office of Basic Energy Sciences, Division of Materials Sciences and Engineering under Award DE-SC0018091. The work was performed in facilities supported by the U.S. Army Research Office and CCDC Army Research Laboratory through the Institute for Soldier Nanotechnologies, under Cooperative Agreement No. W911NF-18-2-0048. Key equipment (the multi-frame camera) was provided through the Office of Naval Research DURIP Grant No. N00014-13-1-0676.

Data Availability

The data that support the findings of this study are available within the article and its supplementary materials or from the corresponding author upon reasonable request.

Supplementary Materials

See supplementary materials for additional post-impact images of rebound craters.

References

[1] C. Borchers, F. Gärtner, T. Stoltenhoff, H. Assadi, and H. Kreye, J. Appl. Phys. **93**, 10064 (2003).
[2] A. Papyrin, V. Kosarev, S. Klinkov, A. Alkimov, and V. Fomin, *Cold Spray Technology* (Elsevier Science, 2006).
[3] Y. Xiong, K. Kang, G. Bae, S. Yoon, and C. Lee, Appl. Phys. Lett. **92**, (2008).
[4] A. Moridi, S.M. Hassani-Gangaraj, M. Guagliano, and M. Dao, Surf. Eng. **30**, 369 (2014).
[5] H. Assadi, H. Kreye, F. Gärtner, and T. Klassen, Acta Mater. **116**, 382 (2016).
[6] J. Bohandy, B.F. Kim, and F.J. Adrian, J. Appl. Phys. **60**, 1538 (1986).
[7] P. Serra and A. Piqué, Adv. Mater. Technol. **4**, 1800099 (2019).
[8] C. Borchers, F. Gärtner, T. Stoltenhoff, and H. Kreye, J. Appl. Phys. **96**, 4288 (2004).
[9] P.C. King, C. Busch, T. Kittel-Sherri, M. Jahedi, and S. Gulizia, Surf. Coatings Technol. **239**, 191 (2014).
[10] M.V. Vidaller, A. List, F. Gaertner, T. Klassen, S. Dosta, and J.M. Guilemany, J. Therm. Spray Technol. **24**, 644 (2015).
[11] H. Assadi, F. Gärtner, T. Stoltenhoff, and H. Kreye, Acta Mater. **51**, 4379 (2003).
[12] W.-Y. Li, C. Zhang, C.-J. Li, and H. Liao, J. Therm. Spray Technol. **18**, 921 (2009).
[13] M. Hassani-Gangaraj, D. Veysset, V.K. Champagne, K.A. Nelson, and C.A. Schuh, Acta Mater. **158**, 430 (2018).
[14] D. Goldbaum, R.R. Chromik, S. Yue, E. Irissou, and J.G. Legoux, J. Therm. Spray Technol. **20**, 486 (2011).
[15] S. Rahmati and B. Jodoin, J. Therm. Spray Technol. **29**, 611 (2020).
[16] V.K. Champagne, M.K. West, M. Reza Rokni, T. Curtis, V. Champagne, and B. McNally, J. Therm. Spray Technol. **25**, 143 (2016).

[17] K.H. Ko, J.O. Choi, and H. Lee, Mater. Lett. **175**, 13 (2016).
[18] M. Hassani-Gangaraj, D. Veysset, K.A. Nelson, and C.A. Schuh, Nat. Commun. **9**, 5077 (2018).
[19] H. Assadi, F. Gärtner, T. Klassen, and H. Kreye, Scr. Mater. **162**, 512 (2019).
[20] M. Hassani-Gangaraj, D. Veysset, V.K. Champagne, K.A. Nelson, and C.A. Schuh, Scr. Mater. **162**, 515 (2019).
[21] M. Hassani-Gangaraj, D. Veysset, K.A. Nelson, and C.A. Schuh, Scr. Mater. **145**, 9 (2018).
[22] M. Hassani-Gangaraj, D. Veysset, K.A. Nelson, and C.A. Schuh, Appl. Surf. Sci. **476**, 528 (2019).
[23] Y. Sun, D. Veysset, K.A. Nelson, and C.A. Schuh, J. Appl. Mech. 1 (2020).
[24] J.-H. Lee, D. Veysset, J.P. Singer, M. Retsch, G. Saini, T. Pezeril, K.A. Nelson, and E.L. Thomas, Nat. Commun. **3**, 1164 (2012).
[25] D. Veysset, S.E. Kooi, A.A. Maznev, S. Tang, A.S. Mijailovic, Y.J. Yang, K. Geiser, K.J. Van Vliet, B.D. Olsen, and K.A. Nelson, J. Mech. Behav. Biomed. Mater. **86**, 71 (2018).
[26] Y. Sun, Y.-C.M. Wu, D. Veysset, S.E. Kooi, W. Hu, T.M. Swager, K.A. Nelson, and A.J. Hsieh, Appl. Phys. Lett. **115**, 093701 (2019).
[27] D. Veysset, A.J. Hsieh, S. Kooi, A.A. Maznev, K.A. Masser, and K.A. Nelson, Sci. Rep. **6**, 1 (2016).
[28] C. Wu, L. Li, and C. Thornton, Int. J. Impact Eng. **28**, 929 (2003).
[29] C.-Y. Wu, L.-Y. Li, and C. Thornton, Int. J. Impact Eng. **32**, 593 (2005).
[30] W. Xie, A. Alizadeh-Dehkharghani, Q. Chen, V.K. Champagne, X. Wang, A.T. Nardi, S. Kooi, S. Müftü, and J.-H. Lee, Sci. Rep. **7**, 5073 (2017).